

Rapid Structural, Kinetic and Immunochemical Analysis of Alpha-Synuclein Oligomers in Solution

William E. Arter^{1,2,†}, Catherine K. Xu^{1,†}, Marta Castellana-Cruz¹,
Therese W. Herling¹, Georg Krainer¹, Kadi L. Saar¹,
Janet R. Kumita¹, Christopher M. Dobson^{1,i} & Tuomas P. J. Knowles^{1,2,*}

¹Department of Chemistry, University of Cambridge, Lensfield Road, Cambridge CB2 1EW
UK

²Cavendish Laboratory, University of Cambridge, JJ Thomson Avenue, Cambridge CB3
0HE, UK

[†]These authors contributed equally

ⁱDeceased September 2019

*Corresponding author. Email tpjk2@cam.ac.uk

Abstract

Oligomers comprised of misfolded proteins are implicated as neurotoxins in the pathogenesis of protein misfolding conditions such as Parkinson's and Alzheimer's diseases. Structural, biophysical, and biochemical characterisation of these nanoscale protein assemblies is key to understanding their pathology and the design of therapeutic interventions, yet is challenging due to their heterogeneous, transient nature and low relative abundance in complex mixtures. Here, we demonstrate separation of heterogeneous populations of oligomeric α -synuclein, a protein central to the pathology of Parkinson's disease, in solution using microfluidic free-flow electrophoresis. We characterise nanoscale structural heterogeneity of transient oligomers on a timescale of seconds, at least two orders of magnitude faster than conventional techniques. Furthermore, we utilise our platform to analyse oligomer ζ -potential and probe the immunochemistry of wild-type α -synuclein oligomers. Our findings contribute to an improved characterisation of alpha-synuclein oligomers and demonstrate the application of microchip electrophoresis for the free-solution analysis of biological nanoparticle analytes.

Keywords

Alpha-synuclein, oligomer, microfluidics, free-flow electrophoresis, aptamer

ⁱ Deceased September 2019

1

2 **Introduction**

3 Protein misfolding is a molecular hallmark of a number of increasingly prevalent human
4 diseases.¹ Amyloid fibrils formed from misfolded proteins are the major components of the
5 Lewy bodies and senile plaques found in the brains of patients with neurodegenerative
6 conditions such as Parkinson's and Alzheimer's diseases, respectively.² However, fibrillar
7 species possess low inherent toxicity themselves, and it is instead pre-fibrillar, oligomeric
8 aggregates that are implicated as the principal cytotoxic agents in these disorders.³⁻⁵ The
9 characterisation and quantitation of these protein nanoparticles in the context of their toxicity
10 and aggregation propensity is therefore an area of intense interest.^{6,7} However, deciphering
11 the structural attributes of oligomeric species, which exist as an intrinsically heterogeneous
12 population of structures during protein aggregation, is hard to achieve using established
13 methods that report the properties of analyte mixtures in an ensemble-averaged manner.
14 Although measurements of oligomer populations, taken throughout protein aggregation
15 processes, have enabled coarse-grained relationships between structure and toxicity to be
16 defined,^{8,9} they do not permit detailed characterisation of oligomer properties including ζ -
17 potential, which may also play a crucial role in determining oligomer aggregation propensity.¹⁰
18 Furthermore, oligomers exist in a complex, dynamic milieu of protein-protein interactions, but
19 current methodologies are often incapable of probing such systems on a timescale relevant to
20 temporal changes in oligomer populations.¹¹ Crucially, current methods for the separation of
21 heterogeneous protein mixtures such as size exclusion chromatography (SEC), analytical
22 ultracentrifugation (AUC) and native gel electrophoresis operate on timescales of minutes to
23 hours, limiting temporal resolution. This feature is particularly important when analysing
24 protein oligomers, since oligomer populations undergo continuous change throughout the
25 aggregation process. In addition, existing techniques for oligomer analysis often perturb the
26 system in question by dilution¹² or use of non-solution state approaches,^{13,14} which may alter
27 the oligomer properties that are observed due to dilution-driven dissociation or interaction with
28 the surface.

29 To address these challenges, we have developed an approach based upon multi-spectral
30 microchip free-flow electrophoresis (μ FFE) that achieves rapid solution-phase fractionation
31 and in-situ analysis of heterogeneous mixtures of protein oligomers and monomers. Our
32 approach enables second timescale separation and solution-phase analysis of oligomer
33 mixtures, at least two orders of magnitude faster than conventional techniques. We focus on
34 the aggregation and oligomerisation of alpha-synuclein (α S), a protein that is strongly
35 implicated in the pathogenesis of Parkinson's disease.¹⁵ Using this approach, complex
36 oligomeric mixtures are fractionated on-chip to afford rapid oligomer quantification and
37 characterisation of ensemble heterogeneity, whilst allowing simultaneous measurement of

1 oligomer ζ -potential, a hitherto inaccessible parameter. In addition, the short experimental
2 timescale (analysis time ~ 5 s), solution-phase conditions and minimal sample dilution enable
3 an accurate, native-state snapshot of dynamic oligomer populations with high temporal
4 resolution.

5 First, we demonstrate the principle of our method through analysis of stable, fluorophore-
6 labelled kinetically trapped α S oligomers that have been characterised in detail previously,¹¹
7 before applying the technique to the analysis of transient oligomers that arise during protein
8 aggregation. Moreover, by use of an oligomer-selective aptamer probe, we further
9 demonstrate the broad applicability of our method by investigation of wild-type, unlabelled α S
10 oligomers.

11 Results and Discussion

12 Our microchip electrophoretic approach is based on a μ FFE^{16,17} platform¹⁸ that allows rapid
13 fractionation of samples containing a complex mixture of oligomeric and monomeric proteins
14 (Figure 1(a)). The sample, flanked by an auxiliary buffer, is passed under laminar flow through
15 the microfluidic chip whilst an electric field is applied perpendicular to the flow direction,
16 resulting in fractionation of the heterogeneous mixture according to the different
17 electrophoretic mobilities of the sample components (Figure 1(b)). Notably, our device
18 incorporates an in-line microfluidic sample-desalting^{19,20} module for rapid (~ 2 s) sample
19 preparation on chip (Figure S1, Supporting Information). This enables the use of high-salt,
20 physiologically-relevant buffers such as phosphate buffered saline (PBS), which are otherwise
21 inaccessible in μ FFE, as excessive ionic conduction through the buffer prevents the
22 application of electric field. To allow facile in-situ differentiation between monomeric and
23 oligomeric α S fractions (Figure 1(b)), α S monomer labelled with a fluorophore (Alexa546)
24 orthogonal to that of the oligomeric protein mixture (Alexa488) is introduced as an in-situ
25 reference. For this approach to be effective, it is necessary for both α S labelling variants to
26 possess the same electrophoretic mobility; hence, the dyes were chosen due to their same
27 inherent charge,²¹ and quantification of the mobilities of the two labelling variants confirmed
28 that they were identical, with $\mu = -1.43 \pm 0.11 \times 10^{-8} \text{ m}^2 \text{ V}^{-1} \text{ s}^{-1}$ (Figure S2). Moreover,
29 comparative analysis of fluorophore-labelled and wild-type α S oligomers by circular dichroism,
30 Fourier transform infra-red spectroscopy and transmission electron microscopy indicated
31 almost identical structural characteristics between the oligomer variants (Figure S4,
32 Supporting Information).

33 We initially demonstrate separation of α S monomers from kinetically-trapped, stable α S
34 oligomers prepared both in high and low-salt conditions (Figure 1(c)). Mixtures of kinetically
35 stable, Alexa488-labelled oligomers together with both Alexa488 and 546-labelled monomer
36 in PBS or 10 mM sodium phosphate buffer were analysed. Two distinct fractions were

1 observed for the oligomeric mixture (Alexa488), but only a single fraction was present for the
 2 monomer-only sample (Alexa546). By comparison to the Alexa546 fluorescence profile, the
 3 lower and higher mobility fractions could be clearly identified as monomeric and oligomeric
 4 protein, respectively (Figure 1(d, e)). As expected, a broad peak width is observed for
 5 monomer, resulting from faster diffusion due to its smaller hydrodynamic radius in comparison
 6 to oligomeric species. Indeed, further analysis revealed significant oligomer heterogeneity,
 7 with a similar electrophoretic profile for both conditions comprising a major oligomer population
 8 at $\mu = -2.49 \pm 0.16 \times 10^{-8} \text{ m}^2 \text{ V}^{-1} \text{ s}^{-1}$ combined with a significant high-mobility shoulder
 9 composed of smaller sub-populations.

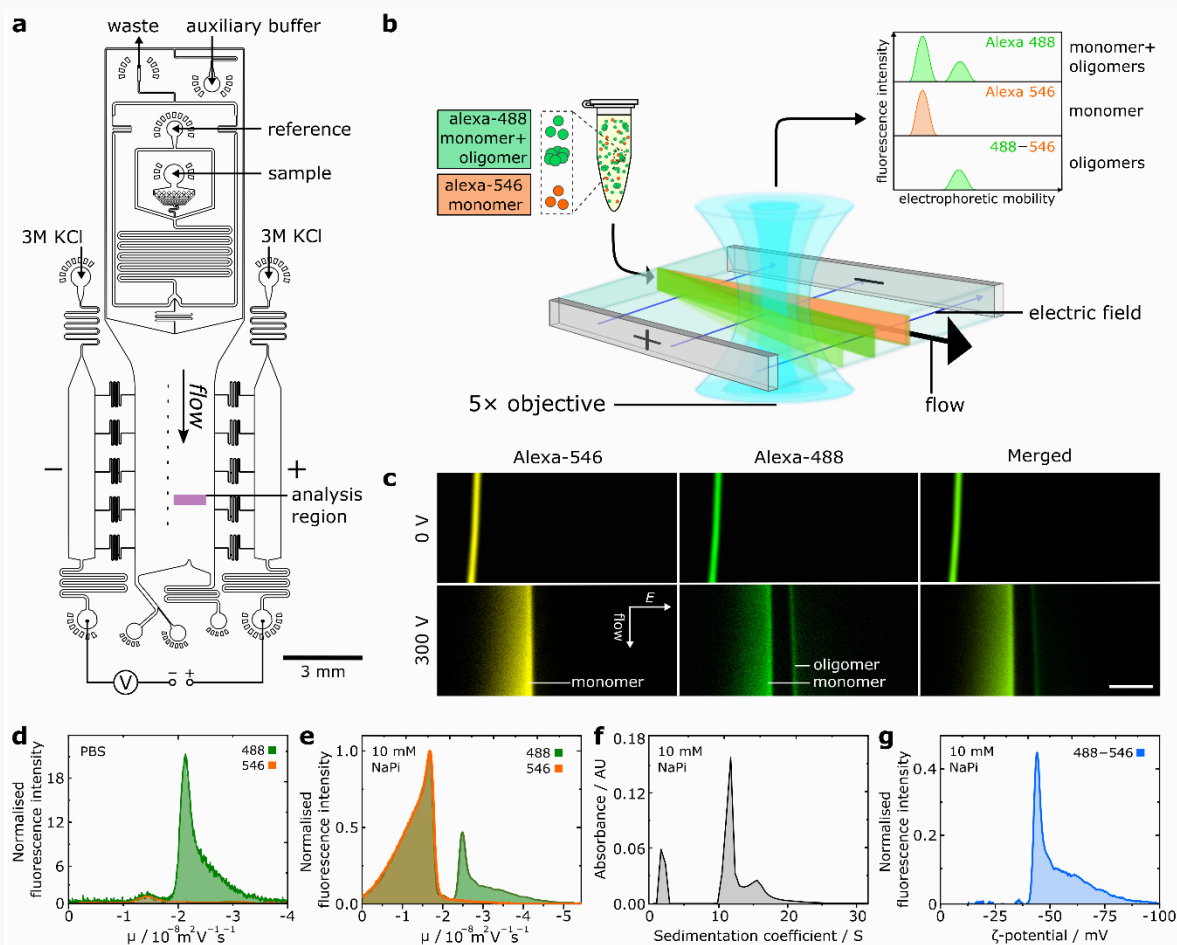
10
 11 We attribute the electrophoretic separation of oligomer and monomer to the faster scaling of
 12 effective oligomer charge relative to oligomer size, for an oligomer of n_m monomer units.
 13 Oligomer electrophoretic mobility (μ_o) is proportional to oligomer charge (q_o) and inversely
 14 proportional to oligomer hydrodynamic radius (r_o) according to $\mu_o \propto \frac{q_o}{r_o} \propto \frac{n_m^\nu}{r_o}$, where ν is a
 15 scaling exponent that links q_o with n_m . α S oligomers have been reported to possess an
 16 approximately spherical morphology,^{11,22,23} and we approximate that $n_m \approx \frac{V_o}{V_m} = \frac{r_o^3}{r_m^3}$ where V_o ,
 17 V_m , r_o and r_m represent the oligomer and monomer volumes and oligomer and monomer
 18 hydrodynamic radii, respectively. Together, these expressions yield the oligomer
 19 electrophoretic mobility as a function of n_m according to Equation 1, where $\nu^* = \nu - \frac{1}{3}$.
 20 According to this relationship, oligomers are expected to have higher mobilities than
 21 monomeric protein, and oligomer mobility is predicted to increase with oligomer size.
 22 Additional data, definition of apparent mobility and further discussion of desalting- μ FFE are
 23 provided in the Supporting Information.

$$24 \quad \mu_o \propto \frac{n_m^\nu}{r_m n_m^{1/3}} = \frac{n_m^{\nu^*}}{r_m} \quad (1)$$

25 To verify this size–mobility relationship, we compared μ FFE to AUC, which is an established
 26 technique for the analysis of size distributions within complex samples. A similar oligomer
 27 profile was consistently observed in both the AUC and μ FFE analyses, indicating a scaling of
 28 oligomer electrophoretic mobility with oligomer size (Figure 1(f), additional data and
 29 rationalisation are provided in the SI). This observation shows that the electropherograms
 30 generated through μ FFE correspond directly to size distributions of component species, as
 31 predicted by Equation 1, thus validating the μ FFE approach as a tool for the analysis of
 32 oligomer structural heterogeneity. From the AUC analysis, values of r_o were found to be in the
 33 range 5.8-11 nm, in agreement with those determined previously.¹¹

1 Having shown that our μ FFE approach enables the fractionation of oligomeric protein
2 mixtures, we analysed the resultant oligomer electropherograms to access oligomer ζ -
3 potentials, a fundamental parameter of nanoscale aggregates. The ζ -potential describes
4 interactions between particles, where it modulates the propensity of the system to aggregate
5 further, and between aggregates and other biological components such as cell membranes.
6 Previously, this parameter has been challenging to study for oligomeric protein aggregates,
7 due to the high degree of structural heterogeneity intrinsic in oligomer samples that confounds
8 conventional techniques, such as dynamic light scattering, for ζ -potential analysis.²⁴ Since our
9 method allows direct observation of oligomer heterogeneity during free-solution
10 electrophoresis, ζ -potentials can be accurately assigned to the major oligomer population
11 rather than to the population average. Following normalisation, the monomer-only Alexa546
12 profile was subtracted from the Alexa488 signal to yield an electropherogram corresponding
13 to oligomeric species only, and values for oligomer ζ -potential were extracted from the
14 reported electrophoretic mobilities (Figure 1(e), see SI).²⁵ The most common oligomer ζ -
15 potential of $\zeta = -42.6 \pm 4.1$ mV is characteristic of particulate systems with high colloidal
16 stability.^{26,27} This finding is significant as it supports the view of protein oligomers as species
17 that do not undergo aggregation themselves.²⁸ The stability we observe suggests that these
18 oligomers will not be removed from solution by flocculation or aggregation, consistent with
19 them existing as a kinetically-trapped,¹¹ long-lived colloidal suspension, with implications for
20 the longevity of oligomer cellular toxicity.^{5,11,29}

21



1
 2 **Figure 1** (a) Schematic of device design for desalting- μ FFE. The device operates through liquid KCl
 3 electrodes, allowing voltage application downstream of the electrophoresis chamber to prevent
 4 disruption of flow by electrolysis products.¹⁸ Reference sample can be introduced on-chip in pure water
 5 diluent, enabling rapid in-situ sample desalting prior to downstream electrophoresis. (b) Schematic for
 6 two-colour microfluidic free-flow electrophoresis of oligomeric α S. (c) Fluorescence images of
 7 Alexa546-labelled α S monomer reference and Alexa488-labelled oligomeric mixture undergoing μ FFE
 8 in 10 mM sodium phosphate (NaPi) buffer (pH 7.4). Direction of fluid flow and electric field (E) shown
 9 by arrows, scale bar = 300 μ m. (d) Electropherograms for Alexa546 monomer reference and Alexa488-
 10 labelled α S oligomeric mixture fluorescence in PBS buffer. (e) Electropherograms for α S monomer and
 11 oligomeric mixture in 10 mM NaPi buffer. (f) AUC data for the same oligomer sample for data shown in
 12 (e), the peak at $S \approx 2$ is due to monomeric protein. (g) Distribution of oligomer ζ -potential.

13
 14 Notably, despite the relationship between surface charge and colloidal stability being of clear
 15 relevance to oligomer behaviour, few experimental studies have attempted to quantify ζ -
 16 potential within heterogeneous oligomer populations, likely due to the challenges such an
 17 experiment would present for established techniques.³⁰ The μ FFE method offers a facile
 18 method for quantifying this parameter in protein aggregation systems, introducing an important
 19 parameter for understanding the physical-chemical nature of aggregate species.

20 Following our analysis of kinetically-trapped, stable oligomers, we applied our μ FFE platform
 21 to the study of transient α S oligomers formed during protein aggregation. Aliquots were

1 periodically withdrawn from the shaking-initiated aggregation reaction of Alexa488-labelled α S
2 monomer, fibrillar components were removed by centrifugation before the samples were
3 analysed by μ FFE. High-mobility fractions in the aggregation mixture corresponding to
4 oligomeric α S could be identified and quantified (Figure 2(a, b, c)), following comparison of
5 the electrophoresis profiles for the aggregation mixture and the Alexa546-labelled monomer
6 reference, which yielded electropherograms corresponding to oligomeric α S alone (Figure
7 2(d)).

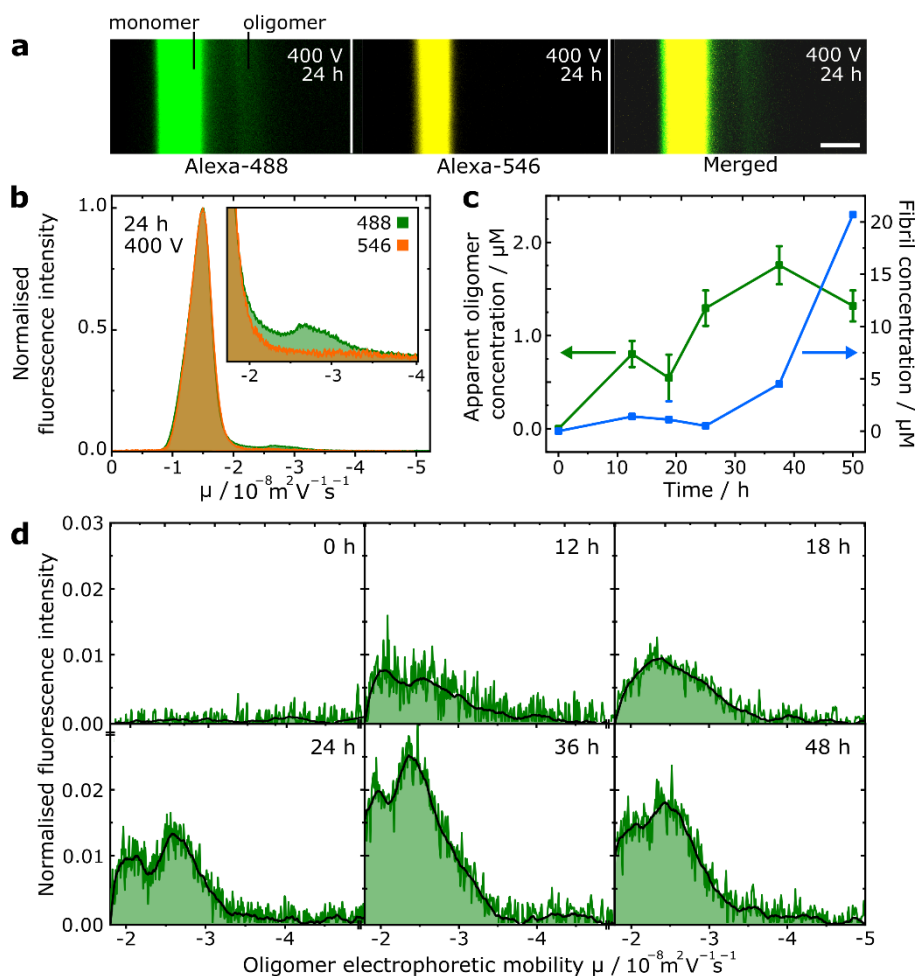
8 No oligomers were observed prior to aggregation initiation, before their concentration
9 increased through the lag phase of the reaction, reaching a peak concentration of 1.75 μ M
10 (monomer equivalent) out of a total α S concentration of 100 μ M with concomitant initiation of
11 protein fibrillisation after 36h. This behaviour is in good agreement with studies employing
12 single-molecule Förster resonance energy transfer (smFRET) experiments.³¹ Furthermore,
13 two distinct oligomeric subpopulations are observable in the aggregation time course, which
14 corresponds well with smFRET experiments where two major subpopulations of α S oligomers
15 have been observed.^{8,9} Oligomers with low FRET efficiency formed first in the aggregation
16 reaction, before converting to species with high FRET efficiency, suggesting a more densely
17 packed structure. Our finding that low mobility species evolve to form high mobility species is
18 thus consistent with an increase in packing efficiency, corresponding to a decrease in
19 hydrodynamic radius.

20 However, smFRET techniques require up to 10^5 -fold sample dilution, which may result in
21 under-sampling of transient, weakly-bound oligomer species that are prone to dissociation.^{12,32}
22 In contrast, sample dilution is not required for μ FFE, enabling accurate oligomer quantitation
23 as evidenced by close agreement with values obtained by other techniques such as size
24 exclusion chromatography.³³ Notably, the μ FFE experiment (\approx 5 s analysis time) is three
25 orders of magnitude faster than methods such as AUC. This crucial feature allowed access to
26 transient species that would be otherwise challenging to observe by AUC or other bulk
27 separation methods, with minimal sample consumption of only a few μ L.

28 In addition to these approaches, previous studies have employed micro-capillary
29 electrophoresis (MCE) techniques^{34,35} to analyse protein aggregation products; these works
30 were primarily focused on the observation of fibrillar species rather than oligomers³⁶ or were
31 non-quantitative.^{37,38} While MCE techniques generally provide advantages in terms of
32 resolution relative to μ FFE,^{39,40} they pose challenges in the quantitation of rare species, due
33 to the injection of a finite volume of sample. In contrast, the steady-state, continuous
34 fractionation process intrinsic to μ FFE prevents sample bleaching during data acquisition and
35 enhances sensitivity through the use of arbitrary exposure time in conventional
36 epifluorescence microscopy. These advantages over MCE techniques are key to our

1 application of μ FPE to detecting and characterising lowly populated oligomeric species in
2 aggregation reactions.

3



4

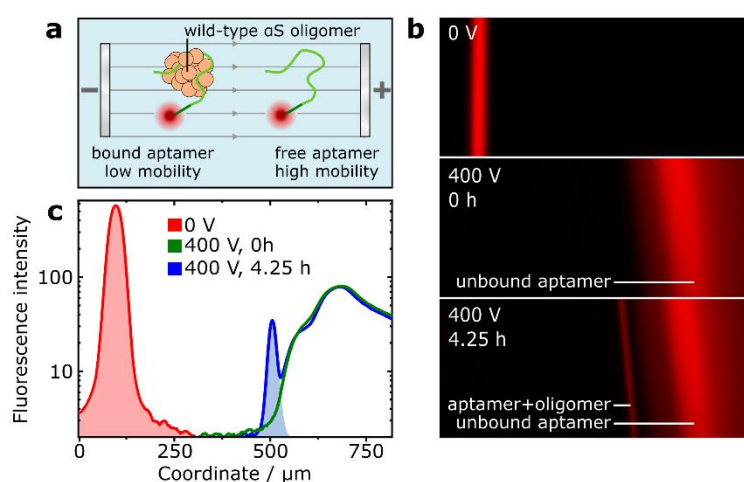
5 **Figure 2** (a) Fluorescence images of μ FPE experiment of transient oligomers formed after 24 h α S
6 aggregation. Scale bar = 300 μm . (b) Superimposed electropherograms of normalised alexa-488 and
7 alexa-546 fluorescence for micrographs shown in (a), (inset) magnification of electropherograms showing
8 oligomeric region. (c) Scatter plot showing progression of oligomer concentration (monomer
9 equivalents) and extent of monomer to fibril conversion (fibril concentration in monomer equivalents)
10 over the sampled time points. Error bars correspond to standard deviation of three repeat
11 measurements of the same sample. (d) Electropherograms and smoothed traces corresponding to
12 oligomeric species only at each sampled aggregation time point.

13

14 Further to the fluorophore-tagged protein systems discussed so far, μ FPE can be employed
15 for the analysis of wild-type oligomeric species when used in conjunction with an appropriate
16 oligomer-binding probe. We demonstrate this capability by utilising a fluorophore-tagged
17 aptamer selective for α S oligomers.⁴¹ As shown previously,⁴² protein–aptamer binding retards
18 the electrophoretic mobility of the aptamer, enabling separation of the bound and unbound
19 fractions (Figure 3(a)). Aliquots taken from stirring-induced aggregation of wild-type α S were

1 incubated with the aptamer and analysed by μ FFE (Figure 3(b)). After 4.25 h aggregation time,
2 an additional fraction at lower mobility than the unbound aptamer was observed. By peak
3 integration and assuming 1:1 binding stoichiometry, an upper bound of 80 nM oligomer
4 concentration could be estimated (Figure 3(c)). By comparison to the maximal monomer-
5 equivalent concentration of labelled oligomer observed previously (Figure 2(c)), it could be
6 approximated that around twenty monomer units are present in each oligomer, in good
7 agreement with previously ascertained values.¹¹ The oligomeric nature of the peak was
8 confirmed by μ FFE of the aptamer in the presence of α S monomer alone and sonicated α S
9 fibrils (Supporting Information). These data show that label-free, wild-type oligomers can be
10 observed and quantified by μ FFE, and demonstrates the versatility of our method towards
11 applications involving immunochemistry-based oligomer detection and manipulation.

12



13

14 **Figure 3** (a) Schematic for fractionation of oligomer-bound and unbound aptamer by μ FFE. (b) Images
15 of aptamer fluorescence during μ FFE, from aptamer mixed into an aggregation reaction of wild-type α S
16 at 0 h and 4.25 h timepoints. Additional, lower-mobility fraction after 4.25 h indicates aptamer-oligomer
17 binding. (c) Analysis and integration of aptamer electropherograms enable approximation of the
18 concentration of aptamer-bound oligomers.

19

20 Conclusion

21 Oligomeric proteins are heavily implicated as toxic agents in protein-misfolding diseases.
22 Understanding oligomer structure, heterogeneity, and physical properties in solution
23 conditions is of vital importance to elucidate relationships between oligomer structure and
24 toxicity, and to enable the design of effective therapeutics.

25 The μ FFE platform presented here is a multifaceted tool for the observation and analysis of
26 these pre-fibrillar intermediates in free solution and physiological conditions. Using this
27 approach, we demonstrate characterisation of oligomer structural heterogeneity within
28 populations of both kinetically-stabilised and transient, on-pathway oligomers isolated from

1 aggregation reaction mixtures. Crucially, on-chip sample preparation and the rapid
2 experimental timescale enabled by the μ FFE platform results in minimal sample perturbation
3 and very high temporal resolution. We quantify oligomer zeta-potential, with our results
4 indicating a high degree of oligomer colloidal stability, supporting the view that oligomers are
5 relatively long-lived species with a low propensity to directly aggregate themselves.
6 Significantly, we observe an interaction between wild-type oligomers and an immuno-probe in
7 free solution. These properties are fundamental to both the physical and biological
8 understanding of oligomer behaviour, but are challenging to study using conventional methods
9 due to the intrinsic heterogeneity of oligomer samples.

10 Oligomer μ FFE has many potential applications, such as in the analysis of protein aggregation
11 kinetics, the links between oligomer structure and toxicity, and for screening protein–protein
12 and protein–small molecule interactions in the development of therapeutic interventions for
13 misfolding disease. More broadly, our findings demonstrate the suitability of free-flow
14 electrophoretic methods for the quantitative, free-solution analysis of nanoparticle analytes in
15 general, according to their size and surface properties.

16 **Supporting Information**

17 Additional methods, detail concerning the microfluidic device, control experiment data,
18 additional experimental data, theoretical basis for this work, and oligonucleotide sequences
19 are provided in the Supporting Information.

20 **Author Contributions**

21 W.E.A, C.K.X, J.R.K, C.M.D, T.P.J.K designed research, W.E.A, C.K.X performed research,
22 M.C.C, T.W.H, K.L.S contributed reagents/analytic tools, W.E.A, C.K.X analyzed data and
23 W.E.A, C.K.X, G.K, J.R.K, T.P.J.K wrote the paper.

24

25 **Acknowledgment**

26 The research leading to these results has received funding from the European Research
27 Council under the European Union's Seventh Framework Programme (FP7/2007-2013)
28 through the ERC grant PhysProt (agreement 337969) and from the Newman Foundation. W.
29 E. A. acknowledges support from the EPSRC Cambridge NanoDTC, EP/L015978/1. C.K.X
30 acknowledges support from a Herchel Smith Research Studentship. T.W.H. acknowledges
31 support from the Oppenheimer Fund and the BBSRC. G.K. has received funding from the
32 European Research Council under the European Union's Horizon 2020 Framework
33 Programme through the Marie Skłodowska-Curie grant MicroSPARK (agreement n° 841466).

1 K.L.S. acknowledges support from the EPSRC. All authors are supported by the Centre for
2 Misfolding Diseases.

3 **References**

- 4 1. Chiti, F. & Dobson, C. M. Protein Misfolding, Amyloid Formation, and Human Disease:
5 A Summary of Progress Over the Last Decade. *Annu. Rev. Biochem.* **86**, 27–68 (2017).
- 6 2. Masters, C. L. *et al.* Amyloid plaque core protein in Alzheimer disease and Down
7 syndrome. *Proc. Natl. Acad. Sci.* **82**, 4245–4249 (1985).
- 8 3. Haass, C. & Selkoe, D. J. Soluble protein oligomers in neurodegeneration: lessons from
9 the Alzheimer's amyloid β -peptide. *Nat. Rev. Mol. Cell Biol.* **8**, 101–112 (2007).
- 10 4. Benilova, I., Karran, E. & De Strooper, B. The toxic A β oligomer and Alzheimer's
11 disease: an emperor in need of clothes. *Nat. Neurosci.* **15**, 349–357 (2012).
- 12 5. Ingelsson, M. Alpha-Synuclein Oligomers: Neurotoxic Molecules in Parkinson's
13 Disease and Other Lewy Body Disorders. *Front. Neurosci.* **10**, 408 (2016).
- 14 6. Bengoa-Vergniory, N., Roberts, R. F., Wade-Martins, R. & Alegre-Abarrategui, J.
15 Alpha-synuclein oligomers: a new hope. *Acta Neuropathol.* **134**, 819–838 (2017).
- 16 7. Ono, K. The Oligomer Hypothesis in α -Synucleinopathy. *Neurochem. Res.* **42**, 3362–
17 3371 (2017).
- 18 8. Cremades, N. *et al.* Direct observation of the interconversion of normal and toxic forms
19 of α -synuclein. *Cell* **149**, 1048–59 (2012).
- 20 9. Ilijina, M. *et al.* Kinetic model of the aggregation of alpha-synuclein provides insights into
21 prion-like spreading. *Proc. Natl. Acad. Sci. U. S. A.* **113**, E1206-15 (2016).
- 22 10. Li, X. *et al.* Early stages of aggregation of engineered α -synuclein monomers and
23 oligomers in solution. *Sci. Rep.* **9**, 1734 (2019).
- 24 11. Chen, S. W. *et al.* Structural characterization of toxic oligomers that are kinetically
25 trapped during α -synuclein fibril formation. *Proc. Natl. Acad. Sci. U. S. A.* **112**, E1994–
26 2003 (2015).
- 27 12. Whiten, D. R. *et al.* Single-Molecule Characterization of the Interactions between
28 Extracellular Chaperones and Toxic α -Synuclein Oligomers. *Cell Rep.* **23**, 3492–3500
29 (2018).
- 30 13. Simone Ruggeri, F., Habchi, J., Cerreta, A. & Dietler, G. AFM-Based Single Molecule
31 Techniques: Unraveling the Amyloid Pathogenic Species. *Curr. Pharm. Des.* **22**, 3950–

- 1 3970 (2016).
- 2 14. Pieri, L., Madiona, K. & Melki, R. Structural and functional properties of prefibrillar α -
3 synuclein oligomers. *Sci. Rep.* **6**, 24526 (2016).
- 4 15. Stefanis, L. alpha-synuclein and Lewy pathology in Parkinson's disease. *Cold Spring
5 Harb Perspect Med* **4**, a009399 (2012).
- 6 16. Turgeon, R. T. & Bowser, M. T. Micro Free-Flow Electrophoresis: Theory and
7 Applications. *Anal. Bioanal. Chem.* **394**, 187–198 (2009).
- 8 17. Herling, T. W., Arosio, P., Müller, T., Linse, S. & Knowles, T. P. J. A Microfluidic Platform
9 for Quantitative Measurements of Effective Protein Charges and Single Ion Binding in
10 Solution. *Phys. Chem. Chem. Phys.* **17**, 12161–12167 (2015).
- 11 18. Saar, K. L. *et al.* On Chip Label Free Protein Analysis with Downstream Electrodes for
12 Direct Removal of Electrolysis Products. *Lab Chip* **18**, 162–170 (2018).
- 13 19. Tibavinsky, I. A., Kottke, P. A. & Fedorov, A. G. Microfabricated ultrarapid desalting
14 device for nanoelectrospray ionization mass spectrometry. *Anal. Chem.* **87**, 351–356
15 (2015).
- 16 20. Wilson, D. J. & Konermann, L. Ultrarapid desalting of protein solutions for electrospray
17 mass spectrometry in a microchannel laminar flow device. *Anal. Chem.* **77**, 6887–6894
18 (2005).
- 19 21. Zanetti-Domingues, L. C., Tynan, C. J., Rolfe, D. J., Clarke, D. T. & Martin-Fernandez,
20 M. Hydrophobic Fluorescent Probes Introduce Artifacts into Single Molecule Tracking
21 Experiments Due to Non-Specific Binding. *PLoS One* **8**, (2013).
- 22 22. van Diggelen, F. *et al.* Two conformationally distinct α -synuclein oligomers share
23 common epitopes and the ability to impair long-term potentiation. *PLoS One* **14**, (2019).
- 24 23. Andreasen, M., Lorenzen, N. & Otzen, D. Interactions between misfolded protein
25 oligomers and membranes: A central topic in neurodegenerative diseases? *Biochim.
26 Biophys. Acta - Biomembr.* **1848**, 1897–1907 (2015).
- 27 24. Arosio, P. *et al.* Microfluidic Diffusion Analysis of the Sizes and Interactions of Proteins
28 under Native Solution Conditions. *ACS Nano* **10**, 333–341 (2016).
- 29 25. Doane, T. L., Chuang, C.-H., Hill, R. J. & Burda, C. Nanoparticle ζ -Potentials. *Acc.
30 Chem. Res.* **45**, 317–326 (2011).
- 31 26. Jiang, J., Oberdörster, G. & Biswas, P. Characterization of size, surface charge, and
32 agglomeration state of nanoparticle dispersions for toxicological studies. *J.*

- 1 *Nanoparticle Res.* **11**, 77–89 (2009).
- 2 27. Joseph, E., Singhvi, G., Grumezescu, A. M., *Nanomaterials for Drug Delivery and*
3 *Therapy*, First Edition, Elsevier Science Publishing Inc (2019).
- 4 28. Lashuel, H. A., Overk, C. R., Oueslati, A. & Masliah, E. The many faces of α -synuclein:
5 From structure and toxicity to therapeutic target. *Nature Reviews Neuroscience* vol. 14
6 38–48 (2013).
- 7 29. Danzer, K. M. *et al.* Different species of alpha-synuclein oligomers induce calcium influx
8 and seeding. *J. Neurosci.* **27**, 9220–32 (2007).
- 9 30. Stetefeld, J., McKenna, S. A. & Patel, T. R. Dynamic light scattering: a practical guide
10 and applications in biomedical sciences. *Biophys. Rev.* **8**, 409–427 (2016).
- 11 31. Ilijina, M. *et al.* Nanobodies raised against monomeric α -synuclein inhibit fibril formation
12 and destabilize toxic oligomeric species. *BMC Biol.* **15**, 57 (2017).
- 13 32. Kjaergaard, M. *et al.* Oligomer Diversity during the Aggregation of the Repeat Region
14 of Tau. *ACS Chem. Neurosci.* **9**, 3060–3071 (2018).
- 15 33. Cremades, N. *et al.* Direct Observation of the Interconversion of Normal and Toxic
16 Forms of α -Synuclein. *Cell* **149**, 1048–1059 (2012).
- 17 34. Harstad, R. K., Johnson, A. C., Weisenberger, M. M. & Bowser, M. T. Capillary
18 Electrophoresis. *Anal. Chem.* **88**, 299–399 (2015).
- 19 35. Voeten, R. L. C., Ventouri, I. K., Haselberg, R. & Somsen, G. W. Capillary
20 Electrophoresis: Trends and Recent Advances. *Anal. Chem.* **90**, 1464–1481 (2018).
- 21 36. Picou, R. A. *et al.* Separation and detection of individual A β aggregates by capillary
22 electrophoresis with laser-induced fluorescence detection. *Anal. Biochem.* **425**, 104–
23 112 (2012).
- 24 37. Sabella, S. *et al.* Capillary electrophoresis studies on the aggregation process of β -
25 amyloid 1-42 and 1-40 peptides. *Electrophoresis* **25**, 3186–3194 (2004).
- 26 38. Napp, A. *et al.* Separation and determination of alpha-synuclein monomeric and
27 oligomeric species using two electrophoretic approaches. *Electrophoresis* **39**, 3022–
28 3031 (2018).
- 29 39. Fonslow, B. R. & Bowser, M. T. Optimizing band width and resolution in micro-free flow
30 electrophoresis. *Anal. Chem.* **78**, 8236–8244 (2006).
- 31 40. Zhang, Z., Zhang, F. & Liu, Y. Recent advances in enhancing the sensitivity and
32 resolution of capillary electrophoresis. *J. Chromatogr. Sci.* **51**, 666–683 (2013).

- 1 41. Tsukakoshi, K., Abe, K., Sode, K. & Ikebukuro, K. Selection of DNA Aptamers That
2 Recognize α -Synuclein Oligomers Using a Competitive Screening Method. *Anal.*
3 *Chem.* **84**, 5542–5547 (2012).
- 4 42. Arter, W. E. *et al.* Combining Affinity Selection and Specific Ion Mobility for Microchip
5 Protein Sensing. *Anal. Chem.* **90**, 10302–10310 (2018).

6